Crosslinking and Its Effects on Polyaniline Films

H. H. TAN, K. G. NEOH, F. T. LIU, N. KOCHERGINSKY, E. T. KANG

Department of Chemical and Environmental Engineering, National University of Singapore, Kent Ridge, Singapore 119260

Received 3 November 1999; accepted 2 May 2000

ABSTRACT: Polyaniline base films with varying degrees of crosslinking were cast from *N*-methylpyrrolidinone solutions at different processing temperatures. The effects of crosslinking on the films' physical properties (solubility, surface morphology, tensile strength), doping characteristics, and transport of ions across the films were investigated. The presence of crosslinking in the film significantly decreases its solubility and enhances its strength, but a comparison of the surface anion/N ratio (as determined by X-ray photoelectron spectroscopy) and the bulk anion/N ratio (as determined from elemental analysis) shows that uniform doping of the crosslinked film by acids is much more difficult to achieve. The transport of H^+ ions through the base film is characterized by an initial time lag followed by a steady-state flux. Both of these parameters are dependent on the degree of crosslinking in the film. It appears that doping of the base film and transport of ions across a doped film are affected differently by crosslinking in the film. © 2001 John Wiley & Sons, Inc. J Appl Polym Sci 80: 1–9, 2001

Key words: polyaniline; crosslinking; solubility; doping characteristics; ion transport

INTRODUCTION

The use of electroactive polymers for practical applications would likely require these polymers to be in the form of films or fibers, rather than the powder form directly obtainable from chemical synthesis. These polymers can be synthesized in film form by electrochemical means but these films generally lack mechanical strength. The chemically synthesized polymers in powder form are soluble in only a limited number of solvents.[1,2] For example, for polyaniline, *N*-methylpyrrolidinone (NMP) is the most effective solvent for this polymer in the base form but not in the salt form doped by common inorganic dopants. The mechanical properties of the polyaniline films cast from an NMP solution can be enhanced when prepared in the gel state and in the presence of crosslinking.[3–5]

In the present work, we investigated the effects of crosslinking on the polyaniline films, in particular, the physical properties, oxidation state, doping characteristics, and ion transport across the film. The latter two parameters are of great importance since these films are cast in the base form which has to be converted to the salt form to be conductive (about 10 orders of magnitude more conductive than the base form[6]). Polyaniline in the 50% oxidized form or emeraldine (EM) was used. A number of techniques were used to characterize the polyaniline to determine the changes which occurred as a result of varying degrees of crosslinking. These techniques include UV-visible absorption spectroscopy, X-ray photoelectron spectroscopy (XPS), atomic force microscopy (AFM), elemental analysis, and measurement of H^+ transport across the films.

EXPERIMENTAL

Synthesis of Films

Polyaniline was prepared via the oxidative polymerization of aniline by ammonium persulfate in

Correspondence to: K. G. Neoh (chenkg@nus.edu.sg).
Contract grant sponsor: National University of Singapore.

Journal of Applied Polymer Science, Vol. 80, 1–9 (2001)

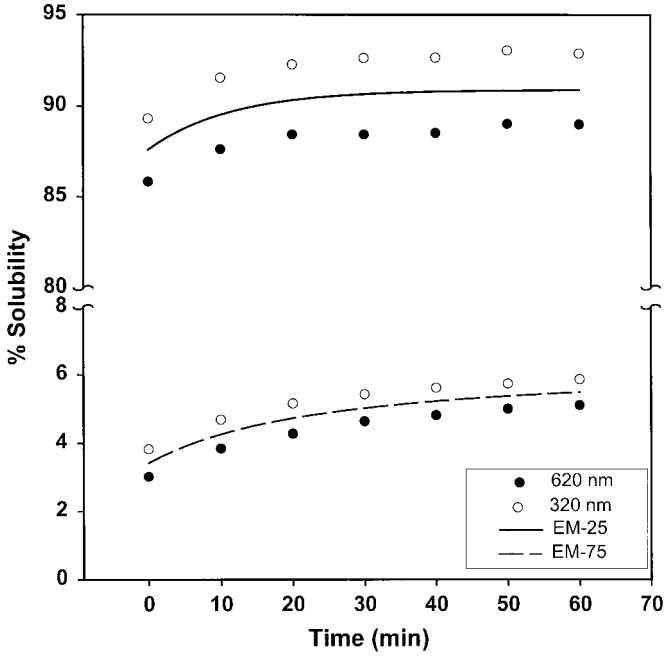

Figure 1 Solubility of EM base film in NMP as a function of time in solution.

1*M* H_2SO_4. The as-synthesized polyaniline salt was deprotonated by treatment with excess 0.5*M* NaOH for 16 h. The resultant polyaniline base (denoted as EM base) was washed with deionized water until the filtrate was neutral and then pumped dry under a dynamic vacuum. The EM base films were prepared from an NMP solution containing 10 wt % EM base powder at a temperature between 25 and 200°C. For films produced at 25°C, the EM base solutions were placed in a dessicator under a dynamic vacuum for 10 h at room temperature to evaporate the NMP. For films prepared at higher temperatures, the EM base solutions were placed in an air-circulated oven maintained at the specified temperature for 6 h, followed by 4 h in a dessicator under a dynamic vacuum at room temperature. The amount of the EM base solution used in each case was calculated to achieve EM base films of about 30 μm in thickness. The EM base films will be denoted as EM-*T*, where *T* is the film processing temperature in °C, for example, EM-25 will represent the EM base film prepared at 25°C, which is the room temperature.

The EM base films were also treated with 1*M* $HClO_4$, toluene-4-sulfonic acid (TSA), and 5-sulfosalicylic acid (SSA), respectively, for 24 h. After this period of treatment, the films were removed, pressed dry between two pieces of filter paper, and dried under a dynamic vacuum for 3 h before being subjected to characterization tests.

Film Characterization

The solubility of the EM base films was determined by comparing the UV-visible absorption of solutions of a known weight of the films in a fixed volume of NMP, with a calibration curve determined using

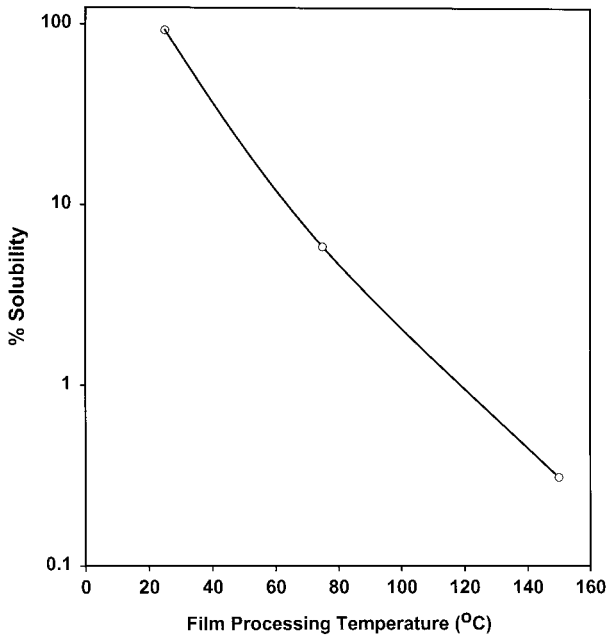

Figure 2 Effect of film processing temperature on the solubility of EM base film in NMP (after 60 min in NMP, based on the absorbance at 320 nm).

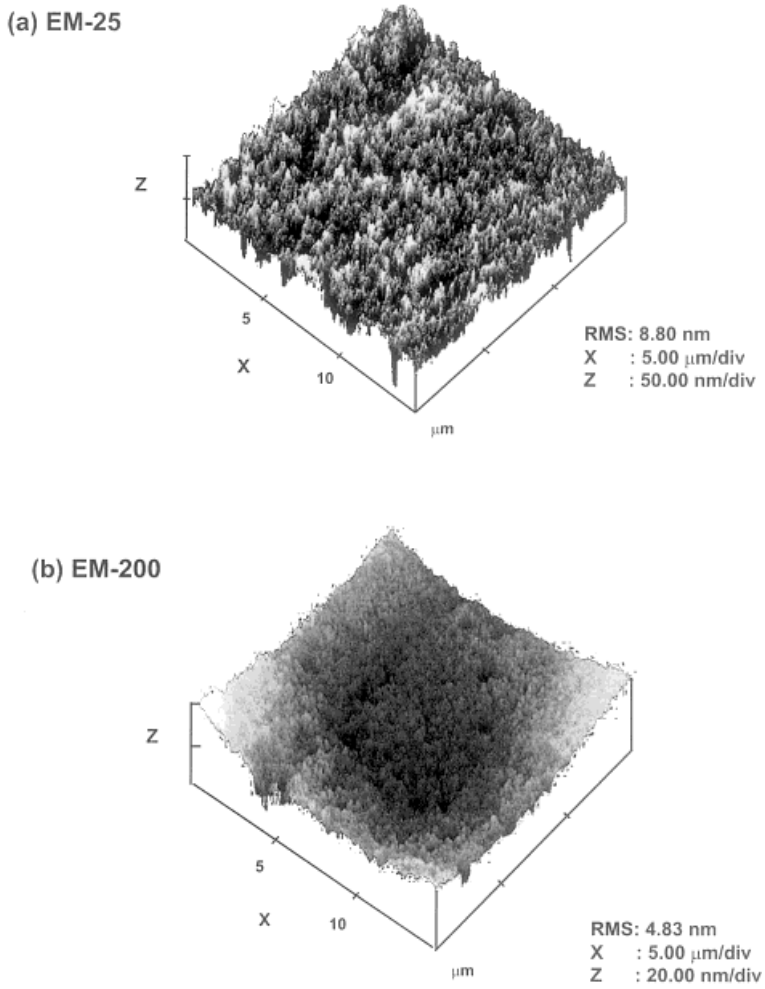

Figure 3 Atomic force micrographs of EM base films processed at different temperatures.

different concentrations of EM base powder in the NMP solution. (The EM base powder was completely soluble in NMP.) Since a certain amount of NMP may be retained in the film,[7] thermogravimetric analysis of the films was carried out in N_2 using a Netzsch STA409 thermal analyzer at a heating rate of 10°C/min to determine the weight of NMP (boiling point of 202°C) retained in the film. The tensile strength of the films was tested under normal ambient conditions using a microprocessor-controlled materials tester, Instron 5544. At least three measurements were taken and the average was reported. The electrical resistance of the film was measured by the two-probe technique and expressed as the sheet resistance, *Rs*, in Ω/sq.[8]

The UV-visible absorption spectroscopy of the EM solution was measured with a Shimadzu UV3101PC scanning spectrophotometer in the wavelength range of 300–900nm. The surface morphology of the films was studied in air using a Nanoscope III scanning atomic force microscope under a constant force mode (scan size 5.0 μm, scan rate 0.5 Hz, set point 3.34 V). The surface compositions of the films were measured using X-ray photoelectron spectroscopy (XPS) on a VG ESCALAB MK II spectrometer with a MgKα X-ray source (1253.6 eV photons). The X-ray source was run at a reduced power of 120 W (12 kV and 10 mA). The core-level spectra were obtained at a photoelectron take-off angle of 75°, measured with respect to the film surface. The pressure in the analysis chamber was maintained at 10^{-8} mbar or lower during the measurements. To compensate for surface-charging effects, all binding energies were referenced to the C1*s* neutral carbon peak at 284.6 eV. In spectral deconvolution,

the full-width at half-maximum of the peak components in a spectrum was kept constant. Surface chemical compositions were determined from peak area ratios corrected with the appropriate experimentally determined sensitivity factors and are accurate to ±10%. The bulk analysis of the C, H, N, and S of the films was carried out with a Perkin–Elmer Series II CHNS analyzer while the Cl content was determined using a titration technique.

The transport of H^+ ions across the EM base films was measured by monitoring the pH change with time of a 0.005*M* KH_2PO_4 buffer solution, which was separated from a 0.1*M* HCl solution by the EM base film. The experimental setup was described in an earlier publication.[9]

RESULTS AND DISCUSSION

Physical Properties

The UV-visible absorption spectra of NMP solutions of EM base films exhibit two absorption bands at 320 and 620 nm. These two absorption bands correspond to the π–π^* transition and the exciton band of EM base, respectively.[10] By comparing the absorbance of the NMP solution of a known weight of EM base film at these two wavelengths with those of a calibration curve determined using different concentrations of EM base powder in NMP, the solubility (defined as weight of EM base in solution per unit weight of film) can be determined. Figure 1 shows the solubility of EM-25 and EM-75 films determined using the absorbance at 320 and 620 nm as a function of the time in solution. As can be seen from this figure, the solubility calculated using the absorbance at the two different wavelengths agree to within 10%, with the value calculated at 320 nm being consistently higher. For the EM-25 film, the solubility curve reaches an asymptotic value of about 0.9 after 60 min. An increase in the film processing temperature from 25 to 75°C causes a drastic decrease in solubility. The effect of processing temperature on solubility is clearly shown in Figure 2. For a processing temperature above 150°C, the soluble fraction is insignificant. Since thermogravimetric analysis showed that there is NMP retained in the films (about 12% NMP in the EM-25 film) and the amount decreases with increase in the processing temperature, the solubility data in Figures 1 and 2 were corrected for the amount of NMP retained in the film.

The three-dimensional atomic force microscopy (AFM) images of EM-25 and EM-200 films are shown in Figure 3(a,b), respectively. It was earlier postulated that the NMP retained in EM base films cast from the NMP solution acts as a plasticizer and the interaction of the NH groups in EM with the C═O groups in NMP leads to an isotropic film with a smooth surface morphology.[11] The AFM image in Figure 3(a) indeed shows that EM base films process a smooth surface morphology. It was also shown earlier that the extraction of NMP by tetrahydrofuran from the surface region of the EM films gives rise to a fibrilar morphology.[11] In the present work, however, a comparison of the surface roughness of the EM base films as indicated by the root-mean-square (RMS) roughness value indicates that the roughness decreases slightly as the processing temperature increases, that is, as the amount of NMP decreases with increasing processing temperature, the roughness of the EM base film actually shows a decrease instead of an increase. Thus, the effects of crosslinking compensate for any increase in roughness which may arise due to the loss of hydrogen bonding as the NMP content decreases.

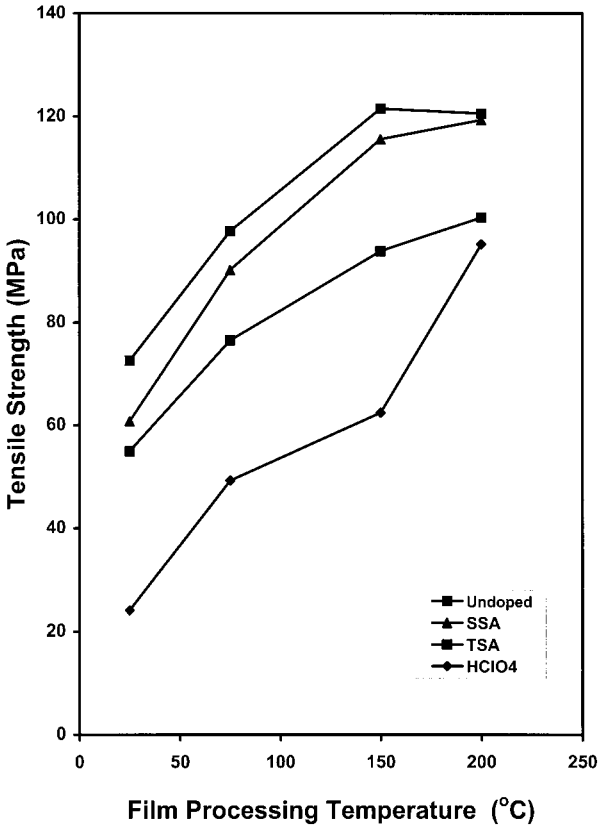

Figure 4 Effect of film processing temperature and acid treatment on the tensile strength of EM films.

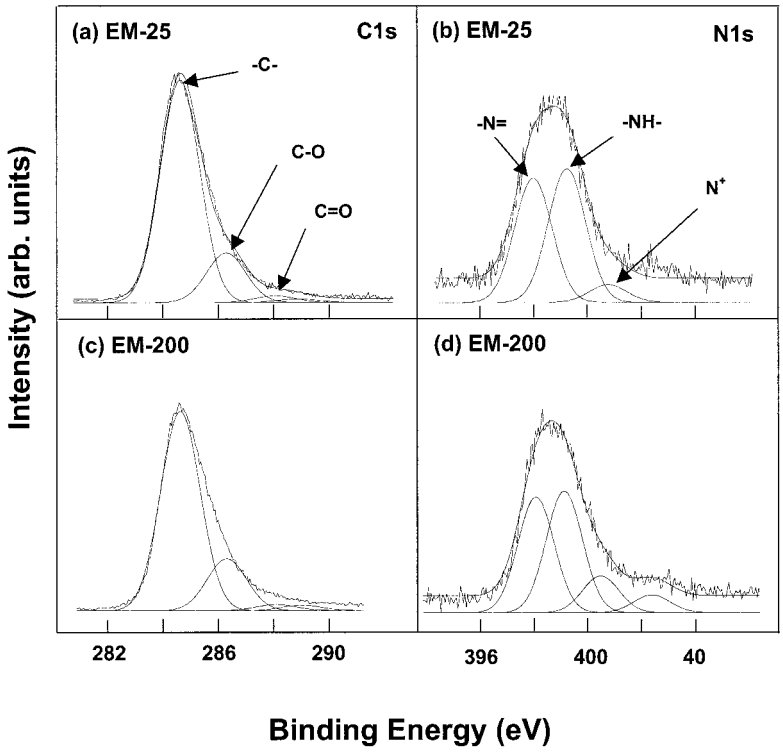

Figure 5 C1*s* and N1*s* XPS core-level spectra of (a,b) EM-25 film and (c,d) EM-200 film.

The maximum tensile strength of the different EM base films at breakpoint is shown in Figure 4. A very significant increase in tensile strength (~60%) is obtained when the processing temperature is increased from 25 to 150°C. The maximum achievable tensile strength of over 100 MPa is higher than that of crosslinked polystyrene (55–70 MPa).[12] But an increase in temperature beyond 150°C does not result in a further increase in the tensile strength. A similar trend was observed when EM-25 base films (prepared at 25°C) were heated to various temperatures.[13] In that case, the tensile strength first shows an increase with temperature to 150°C and then a sharp decrease beyond that temperature. This decrease was attributed to the degradation of the EM polymer.[13]

Oxidation State and Doping Characteristics

The major C and N species on the surface of the films can be readily determined from the deconvoluted XPS C1*s* and N1*s* core-level spectra, respectively. The deconvolution was carried out using previously established peak assignments [as indicated by the binding energy (BE)] for the various C and N species.[13,14] Figure 5 shows a comparison of the C1*s* and N1*s* spectra of the EM-25 and EM-200 base films. It is clear from Figure 5(a,c) that the proportions of the oxidized C, that is, C—O (BE of 286.2 eV), C═O (BE of 287.9 eV), and O—C═O (BE of 288.7 eV) species, do not increase with increase in the processing temperature. On the other hand, the proportion of the N^+ group (BE $\geq$ 401 eV) increases as the film processing temperature increases [Fig. 5(b,d)]. The detailed XPS results are given in Table I. The increase in the N^+ species is likely to be due to the formation of either surface oxidation products or charge-transfer products of nitrogen with oxygen, since these processes are promoted during the long exposure to oxygen at elevated temperature. Alternatively, the crosslinking reactions may give rise to N—N species. Depending on the nature of these species, the BE of the peak components attributable to these species may range from 398 to >402 eV.[15]

The bulk C/N, H/N, and O/N ratios determined from elemental analysis are also given in Table I. The C/N ratio is fairly constant, whereas the H/N ratio shows a very substantial decrease as the

Table I Surface and Bulk Compositions of EM Base Films After Different Degrees of Crosslinking

	Surface Composition				Bulk Composition		
EM Base Film	C[a]/C	—N═/N	—NH—/N	N^+/N	C/N	H/N	O[b]/N
EM-25	0.79	0.45	0.49	0.06	5.82	5.50	0.58
EM-75	0.75	0.39	0.53	0.08	5.90	4.95	0.45
EM-150	0.74	0.35	0.53	0.12	5.97	4.89	0.37
EM-200	0.76	0.39	0.42	0.19	5.68	3.70	0.37

[a] C bonded to C, N, or H.
[b] Oxygen content calculated from the difference between the total weight and the weight contributed by C, H, and N.

processing temperature increases. For an idealized EM base, the H/N ratio is expected to be 4.5. The higher H/N ratio observed for the EM-25 film is likely to be partially due to the NMP (H/N = 6) and water retained in the film. The combination of hydrogen from these sources will diminish with increase in processing temperature. For EM-200, the decrease in the H/N ratio to less than the value expected of the EM base is postulated to be due to crosslinking between the chains, resulting in the loss of hydrogen. The decrease in the O/N ratio with processing temperature is also consistent with a decreasing amount of NMP and water retained in the film as the processing temperature increases.

The treatment of EM base film with acids is expected to result in the protonation of the —N═ units to the N^+ species.[14] The XPS N1*s* core-level spectra of the EM base films after acid ($HClO_4$, TSA, SSA) treatment indicate that all the surface —N═ units (BE at 398.2 eV) are readily protonated, even for base films prepared at 200°C. Figure 6 shows the N1*s* core-level spectra of EM-25 and EM-200 films after treatment with $HClO_4$ for 24 h. In Figure 6(a), the complete absence of the —N═ peak and the greatly diminished —NH— peak (BE of 399.4 eV) coupled with the predominant N^+ peak (N^+/N = 0.88) indicate that not only are the —N═ units completely protonated but a substantial fraction of the —NH— units were converted to N^+ as well.[16] For the EM-200 film [Fig. 6(b)], the results indicate that the N^+ species (N^+/N = 0.49) are formed primarily from the —N═ groups. This observation that the —NH— units in the EM base films prepared at the lower temperatures are more prone to protonation than are the ones prepared at 200°C was also made when TSA and SSA were used. The presence of the ClO_4^- or $—SO_3^-$ anions in the protonated films is ascertained by the peak at 207 eV in the Cl2*p* core-level spectra[17] or the peak at 168 eV in the S2*p* core-level spectra,[18] respectively. It was also observed that while the N^+/N and anion/N (i.e., ClO_4^-/N or $—SO_3^-$/N) ratios generally

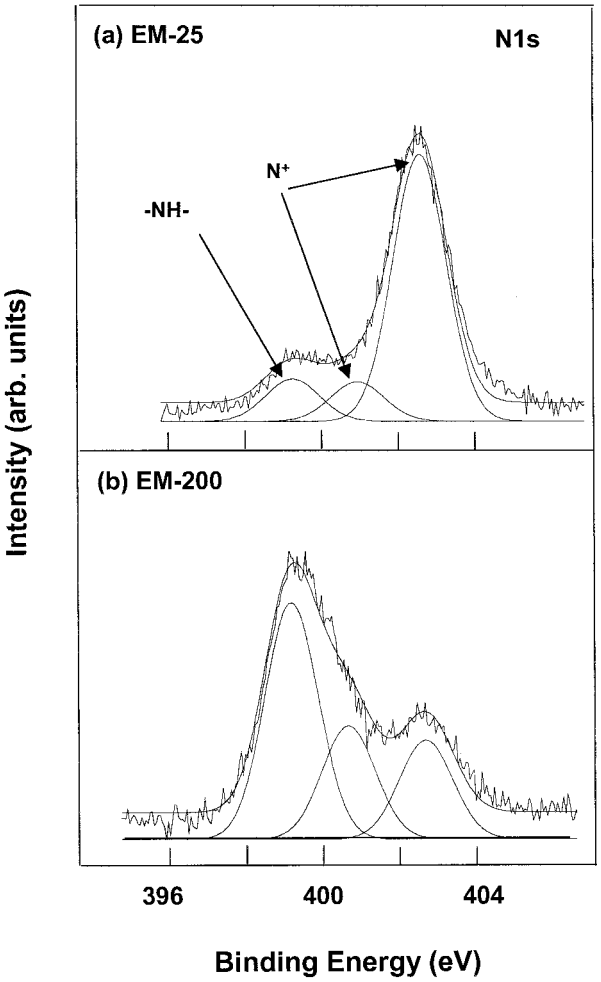

Figure 6 N1*s* core-level spectra of (a) EM-25 after treatment with $HClO_4$ for 24 h and (b) EM-200 after treatment with $HClO_4$ for 24 h.

show good agreement (within 5–10%) for the films prepared at the lower temperatures, the difference between these ratios for the EM-200 film increases to 20% or more. This corroborates the postulate mentioned earlier that a portion of the N^+ species in the EM-200 film are associated with surface oxidation or charge-transfer products with oxygen.

Although the XPS results indicated that complete protonation of the —N═ groups for all the films by the three acids tested is possible, the difference in the color of the films prepared at different temperatures after acid treatment as well as the films treated by different acids give the first indication that the extent of doping in the bulk varies greatly among the films. A measure of the extent of doping in the bulk of the film is provided by the bulk Cl/N or S/N mol ratio (as determined by elemental analysis). This is given in Table II for the films prepared at the four temperatures and treated by the three acids of 1*M* concentration for 24 h. From Table II, it can be seen that for a film prepared at any particular temperature the extent of dopant penetration into the bulk of the film decreases in the order $HClO_4$ > TSA > SSA. A Cl/N or a S/N mol ratio of 0.5 would indicate that all the —N═ units of the EM base film (50% —N═ units) are protonated with either ClO_4^- or $—SO_3^-$ anions serving as counterions. This is indeed the case for the EM-25 film treated with 1*M* $HClO_4$ for 24 h. On the other hand, for the SSA-treated EM-25 film, the surface S/N ratio as determined by XPS is 0.49, whereas the bulk S/N ratio is 0.02, indicating minimal doping in the bulk. This illustrates the extremely slow diffusion of the SSA ions into the bulk of the film even when there is minimal crosslinking.

From Table II, it is also clear that as the processing temperature of the film increases the bulk anion/N ratio decreases regardless of the acid used. Thus, with an increasing extent of crosslinking in the film, the morphology of the film has been sufficiently altered such that the migration of ions through the film is impeded. As a direct result of the different extents of doping achievable for the different EM films, the resistivities of these films are also vastly different, as shown in Figure 7. The migration of the dopants into the bulk of the film results in decrease in the tensile strength, as shown in Figure 4. When SSA is used, there is negligible migration of the dopant into the bulk of the film (Table II) and the tensile strengths of all such films are close to those of the base films. When $HClO_4$ is used, the bulk of EM-25 film is more readily accessible to the dopant molecules, and the tensile strength decreases from about 73 MPa for EM-25 to 24 MPa after treatment. However, as the ability of the dopant molecules to migrate into the bulk of the film greatly diminishes when the processing temperature increases beyond 150° (a comparison of the EM-150 and EM-200 results is shown in Table II), the tensile strength of the $HClO_4$-treated EM-200 film is significantly higher than is the correspondingly treated EM-150 film (Fig. 4), in contrast to the EM-150 and EM-200 films before acid doping.

Table II Bulk Cl/N or S/N Mol Ratios for EM Film after Acid Treatment for 24 h

	Cl/N or S/N		
EM Film	$HClO_4$	TSA	SSA
EM-25	0.50	0.37	0.02
EM-75	0.46	0.33	0.02
EM-150	0.35	0.01	0.01
EM-200	0.10	0.01	0.003

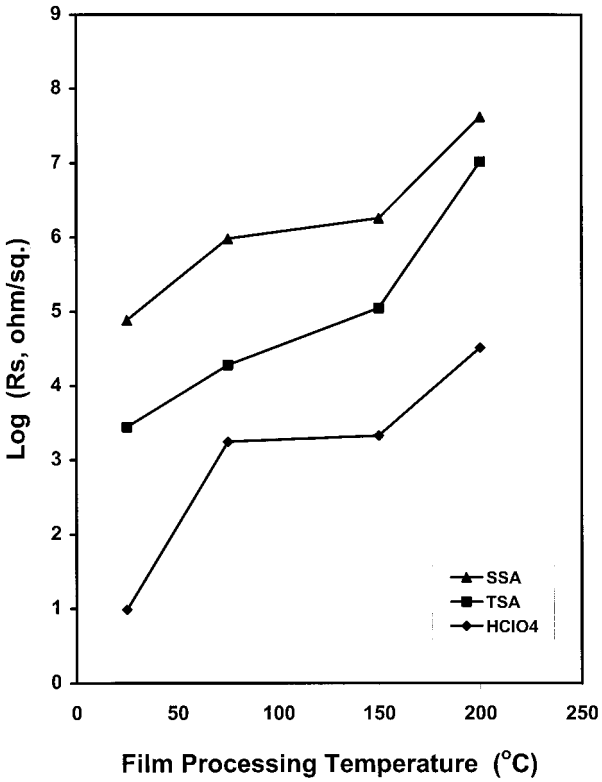

Figure 7 Effect of film processing temperature and acid treatment on sheet resistance of EM films.

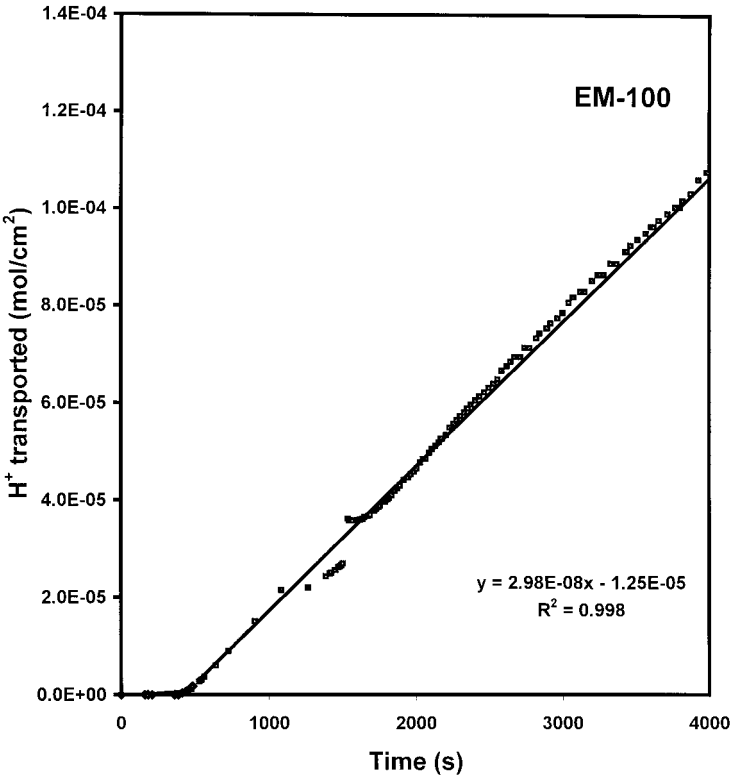

Figure 8 Transport of H^+ ions across EM-100 film as a function of time.

Transport Properties

The comparison of the surface and bulk anion/N ratio in Table II provides a good, albeit indirect, indication of the resistance of the film to the migration of the ions. This transport resistance is better quantified by the measurement of the flux of H^+ ions transported across the film from a HCl solution to a phosphate buffer. Figure 8 shows the amount of H^+ ions transported across the EM-100 base film per unit area of film as a function of time. The features of this plot are typical of those obtained with the other EM base films, and these plots are characterized by an initial time lag followed by a linearly increasing portion. The time lag characterizes the time required to achieve steady state (i.e., constant rate) H^+ transport through the film and the steady-state flux of the H^+ ions through the film can be calculated from the slope of the linear portion. Figure 9(a,b) shows the effect of the film processing temperature on the initial time lag and the flux of the H^+ ions through the films, respectively. As H^+ ions coupled with Cl^- ions are transported through the EM base film, the interaction of these ions with the —N═ groups changes the EM from the undoped base to the doped state. Since H^+ ions become bonded to the —N═ groups and the Cl^- anions act as counterions to the resulting N^+, the EM base film acts as a sink for these ions and the time lag may be viewed as the time taken for the propagation of the reaction front between the doped and undoped regions. From Figure 9(a), it can be seen that the time lag increases slightly when the processing temperature increases from 25 to 100°C and very substantially for temperatures higher than 100°C.

Figure 9(b), on the other hand, shows that the detrimental effect of film processing temperature on the steady-state transport rate is obvious upon raising the processing temperature above 25°C. This is consistent with the solubility data in Figure 2 which indicates that crosslinking is significant even if the film processing temperature is increased to 75°C only. The differing shape of the curves in Figures 9(a,b) is an indication that the two processes, progression of doping through the base film versus the transport of ions through a doped film, are affected differently by crosslinking in the film, that is, the first process is determined by the slow structural transitions of the polymer from the undoped to the

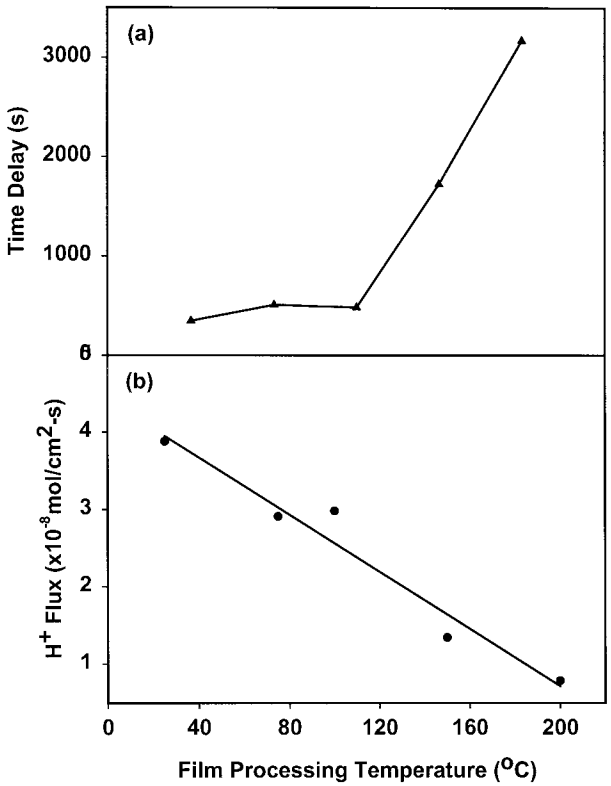

Figure 9 Effect of film processing temperature on (a) time delay and (b) rate of H^+ transport across EM base films.

doped configurations, while at the steady state the transport of H^+ is dependent on the local microviscosity of the polymer which increases as a result of crosslinking.

CONCLUSIONS

Polyaniline base films of increasing degrees of crosslinking were made by heating solutions of EM base in NMP to dryness at increasing temperature. Films processed at room temperature can almost be entirely redissolved in NMP while those processed at 200°C are essentially insoluble in this solvent. As the degree of crosslinking in the base film increases, the process of converting the base films to salt films by redoping with acids becomes increasingly difficult even for inorganic acids. As a result, the resistivity and tensile strength of the redoped films are highly dependent on the degree of crosslinking as well as on the acid used for the redoping process. The transport of H^+ ions across the film is characterized by an initial time lag and a steady-state flux. The initial time lag representing the propagation of the reaction front between the doped and undoped regions in the film shows a very significant increase for films processed above 100°C, while the steady-state flux of H^+ ions is a decreasing function of the degree of crosslinking.

The authors gratefully acknowledged the assistance of Mr. Lei Wen in the transport experiments. This work was supported by a research grant from the National University of Singapore.

REFERENCES

1. Angelopoulous, M.; Asturias, G. E.; Elmer, S. P.; Ray, A.; Scherr, E. M.; MacDiarmid, A. G.; Akhtar, M.; Kiss, Z.; Epstein, A. J Mol Cryst Liq Cryst 1988, 160, 151.
2. Cao, Y.; Heeger, A. J. Synth Met 1993, 52, 193.
3. Tzou, K.; Gregory, R. V. Synth Met 1993, 55–57, 983.
4. Oka, O.; Kiyohara, O. Synth Met 1993, 55–57, 999.
5. Kitani, A.; Yoshioka, Y.; Sasaki, K. Synth Met 1993, 55–57, 3566.
6. MacDiarmid, A. G.; Chiang, J. C.; Richter, A. F.; Epstein, A. J. Synth Met 1987, 18, 285.
7. Neoh, K. G.; Kang, E. T.; Tan, K. L. J Macromol Sci Pure Appl Chem A 1992, 29, 401.
8. Jaeger, R. C. In Introduction to Microelectronic Fabrication; Neudeck, G. W.; Pierret, R. F., Eds.; Addison-Wesley: Reading, MA, 1993, p 66.
9. Lei, W.; Kocherginsky, N..M. J Membr Sci 2000, 167, 135.
10. Cao, Y.; Smith, P.; Heeger, A. J. Synth Met 1989, 32, 263.
11. Chen, S. A.; Lee, H. T. Macromolecules 1993, 26, 3254.
12. Product Catalogue of Goodfellow Cambridge Ltd.; Cambridge Science Park, Cambridge, UK, 1998/99; p 532.
13. Li, Z. F.; Kang, E. T.; Neoh, K. G.; Tan, K. L. Synth Met 1997, 87, 45.
14. Tan, K. L.; Tan, B. T. G.; Kang, E. T.; Neoh, K. G. Phys Rev B 1989, 39, 8070.
15. Handbook of X-ray Photoelectron Spectroscopy; Chastain, J., Ed.; Perkin–Elmer: Eden Prarie, MN, 1992; p 227.
16. Neoh, K. G.; Kang, E. T.; Tan, K. L. J Phys Chem 1997, 101, 726.
17. Pfluger, P.; Street, G. B. J Chem Phys 1984, 80, 544.
18. Handbook of X-ray Photoelectron Spectroscopy; Chastain, J., Ed.; Perkin–Elmer: Eden Prarie, MN, 1992; p 236.